Journal of Applied Polymer Science

# Dual-stimuli-responsive polymer-coated mesoporous silica nanoparticles used for controlled drug delivery

**Mei-Yan Yang,[1] Lei Tan,[1] Hai-Xia Wu,[1,2] Chuan-Jun Liu,[1] Ren-Xi Zhuo[1]**

[1]Key Laboratory of Biomedical Polymers of Ministry of Education, College of Chemistry and Molecular Science, Wuhan University, Wuhan 430072, People's Republic of China

[2]College of Chemistry and Chemical Engineering, Luoyang Normal University, Luoyang 471022, People's Republic of China

Correspondence to: C. J. Liu (E-mail:cjliu@whu.edu.cn)

**ABSTRACT:** In this article, a temperature- and pH-responsive delivery system based on block-copolymer-capped mesoporous silica nanoparticles (MSNs) is presented. A poly[2-(diethylamino)ethyl methacrylate)] (PDEAEMA)-*b*-poly(*N*-isopropyl acrylamide) (PNIPAM) shell on MSNs was obtained through the surface-initiated atom transfer radical polymerization. The block copolymer PDEAEMA-*b*-PNIPAM showed both temperature- and pH-responsive properties. The release of the loaded model molecules from PDEAEMA-*b*-PNIPAM-coated MSNs could be controlled by changes in the temperature or pH value of the medium. The as-desired drug-delivery carrier may be applied to biological systems in the future. © 2015 Wiley Periodicals, Inc. J. Appl. Polym. Sci. **2015**, *132*, 42395.

**KEYWORDS:** biomaterials; drug-delivery systems; nanoparticles; nanowires and nanocrystals; stimuli-sensitive polymers

Received 10 December 2014; accepted 21 April 2015

**DOI: 10.1002/app.42395**

## INTRODUCTION

Smart drug-delivery systems have attracted much attention in the past few decades.[1,2] Significant efforts have been devoted to the creation of an ideal nanocarrier.[3–5] In recent years, various nanocontainers that can controllably trap and release guests have been designed for drug delivery; these containers include micelles,[6,7] vesicles,[8,9] and nanogels.[10–12] However, the issue of stability is still a great challenge to nanocarriers[13,14] and may induce the preleakage of drugs and uncontrolled drug delivery. Inorganic nanoparticles, such as nanotubes, nanoshells, and mesoporous nanoparticles, can be more stable than organic materials.[3] Compared with nonporous materials, mesoporous silica nanoparticles (MSNs) provide a higher drug-loading capacity. A variety of stimuli-responsive gatekeepers have been developed for MSN-based controlled drug-delivery systems; these include inorganic nanoparticles,[15] peptide molecules,[16] polymers,[17–19] and molecular valves.[20] The stimuli applied for on-demand drug-delivery systems can include temperature,[21] light,[22] magnetic forces,[23,24] pH,[25–28] oxidation–reduction,[29,30] enzymes,[17,18] and so forth. As reported by Zhu *et al.*,[31] ZnO quantum dots were introduced to block the nanopores of MSNs. Within the acidic intracellular microenvironment of cancer cells, ZnO quantum dot lids on the MSN surface can be dissolved efficiently; this is followed by the rapid release of drug molecules into the cytosol. Pan *et al.*[32] coated the MSNs with a pH-responsive polymer brush made of poly[2-(diethylamino)ethyl methacrylate)] (PDEAEMA). At acidic pH, the guests moved from the MSNs freely, but the pores could be sealed again at pH 8.0. Intensive efforts have been made on the fabrication of multiresponsive MSN systems.[33–35] Gooding *et al.*[36] prepared a dual bioresponsive mesoporous silica nanocarrier for targeted drug-delivery cancer cells; this nanocarrier could respond to pH and esterase.

In this article, we report a well-designed PDEAEMA-*b*-poly(*N*-isopropyl acrylamide) (PNIPAM)-coated nanocontainer based on MSNs (PDEAEMA-*b*-PNIPAM@MSN or $P_2P_1$@MSN) and prepared by sustained surface-initiated atom transfer radical polymerization (SI-ATRP); this nanocontainer could repeatedly respond to different pH and temperature values in the medium. To obtain the desired MSNs, the atom transfer radical polymerization (ATRP) initiator 2-bromoisobutyryl bromide (BIBB) was linked to the surface of the MSNs first; this was followed by the polymerization of the monomer *N*-isopropyl acrylamide (NIPAM) and 2-(diethylamino)ethyl methacrylate (DEAEMA) step by step. As a result, the well-defined core–shell structure MSNs were prepared. At a low temperature and high pH value, the model molecule Rhodamine B (RhB) was sealed in the pores of the MSNs, whereas the release rate of the guests was largely promoted when it encountered higher temperature and lower pH values. Furthermore, the release of RhB could be controlled repeatedly by adjustment of the temperature and pH values in solution.

Additional Supporting Information may be found in the online version of this article.

## EXPERIMENTAL

### Materials

Cetyl trimethyl ammonium bromide (CTAB), tetraethyl orthosilicate, and potassium biphthalate were provided by Sinopharm Chemical Reagent Co., Ltd. (Shanghai, China) and were used as received. DEAEMA (98%), 3-aminopropyl triethoxysilane (APTES; 98%), BIBB (98%), *N,N,N′,N″,N″*-pentamethyl diethylenetriamine (PMDETA; 99%), and NIPAM (98%) were purchased from Aladdin Reagent Co., Ltd. NIPAM was purified by recrystallization from hexane and dried *in vacuo* at 45°C before use. CuBr was treated with glacial acetic acid and acetone, washed with ethanol, and dried in a vacuum oven before use. From Tianjin Dalu Chemical Reagent Co., Ltd. (China), NaOH was obtained. Dichloromethane ($CH_2Cl_2$) and anhydrous toluene were treated with calcium hydride and distilled before use. Triethylamine was soaked with a molecular sieve. Fetal bovine serum, Dulbecco's Modified Eagle's Medium (DMEM), Dubelcco's phosphate-buffered saline (PBS), and 3-(4,5-dimethyl thiazol-2-yl)−2,5-diphenyltetrazolium bromide (MTT) were obtained from Invitrogen. COS7 cells were obtained from the Cell Bank of Chinese Academy of Sciences (Shanghai, China). All other reagents and solvents were provided by Sinopharm Chemical Reagent Co., Ltd. (Shanghai, China) and were used without further purification.

### Preparation of the MSNs and the $NH_2$ Modified MSN (MSN-$NH_2$)

The MSNs were prepared with tetraethyl orthosilicate as a silica source and CTAB as template through the generally used base-catalyzed sol–gel method with some modification,[37] as described in the Supporting Information. The obtained MSN (1.94 g) was well dispersed in dry toluene (145 mL) by ultrasound, and then APTES (7.18 mL, 30.67 mmol) was added. The mixture was allowed to conduct for 24 h at 112°C under refluxing. MSN–$NH_2$ was collected by filtration, washed with toluene, ethanol, and dried *in vacuo* at 40°C overnight.

### Removal of the CTAB Template in MSN–$NH_2$

The surfactant template CTAB in the MSN–$NH_2$ was removed through an extraction procedure.[37] MSN–$NH_2$ (1.64 g) was suspended in acidic methanol solution (175 mL) with HCl (9.84 mL, 36%) and then refluxed for 24 h. To acquire MSN–$NH_2$ without CTAB, the mixture was treated by *in vacuo* filtering, washed with methanol, and then dried *in vacuo* at 45°C for 24 h.

### Synthesis of the Initiator Linked MSN (MSN-Br)

The ATRP initiator, BIBB, was covalently connected to MSN–$NH_2$. MSN–$NH_2$ (1.50 g) was dispersed in dry $CH_2Cl_2$ (102 mL);this was followed by the addition of triethylamine (2.40 mL, 17.22 mmol) under ice-bath conditions, and then BIBB (1.60 mL, 12.94 mmol) was slowly added to the mixture. The mixture was kept at 0°C for 2 h and then transferred to room temperature for another 48 h with violent stirring. The resulting solid was separated by filtration. Then, MSN–Br was washed with $CH_2Cl_2$, ethanol, and water. Finally, it was dried *in vacuo* at 45°C overnight.

### Preparation of the PNIPAM-Coated MSN (PNIPAM@MSN or $P_1$@MSN)

The $P_1$@MSN was obtained by ATRP.[38,39] NIPAM (1.18 g, 10.43 mmol), CuBr (15 mg, 0.10 mmol), and PMDETA (65 $\mu$L, 0.30 mmol) were dissolved in a mixture of methanol and water (1 : 1, 5 mL) and dispersed evenly by ultrasound for 5 min. After two freeze–pump–thaw cycles, MSN–Br (250 mg) was quickly added to the degassed solution, and then another two times freeze–pump–thaw cycles were performed to exclude the air absolutely. The polymerization was carried out under an argon atmosphere at room temperature for 24 h and stopped by exposure to air. The PNIPAM@MSN was isolated by centrifugation at 11,000 rpm; repeatedly washed with methanol, $H_2O$, and acetone; and dried at 45°C *in vacuo* overnight.

### Synthesis of PDEAEMA-*b*-PNIPAM@MSN ($P_2P_1$@MSN)

The grafting of DEAEMA to the MSN surface was accomplished by sustained ATRP, which was initiated by a $P_1$@MSN macroinitiator. According to previous published procedures,[32,40] DEAEMA (10.87 mL, 54.45 mmol), CuBr (257.6 mg, 1.80 mmol), and PMDETA (375 $\mu$L, 1.80 mmol) were added to $CH_3OH$ (43 mL) with vigorous stirring. After two freeze–vacuum–argon cycles, the macroinitiator $P_1$@MSN (185 mg) was added to the mixed monomer–catalyst solution. Another two freeze–vacuum–argon cycles were conducted. The reaction was performed at 70°C for 63 h. The polymer-coated MSN PDEAEMA-*b*-PNIPAM@MSN ($P_2P_1$@MSN) was washed through centrifugation (11,000 rpm) with THF and $CH_3OH$ five times and dried at 45°C *in vacuo* overnight.

### Dye Loading and Release

RhB was chosen as a model drug molecule for the study of the release behaviors; RhB was stable under the designed conditions. $P_2P_1$@MSN (51 mg) was added to the PBS solution of RhB (1.37 mg, pH = 4.0, 0.05*M*, PBS, 25 mL) and dispersed by ultrasonication. After stirring for 36 h at room temperature, RhB loaded MSNs (RhB@$P_2P_1$@MSN) were separated from the mixture by centrifugation at 11,000 rpm. To remove the RhB adsorbed on the surface of the particles and prevent premature release, the supernatant was replaced by a fresh alkaline aqueous solution (pH = 8.0, 0.05*M* PBS) until the fluorescence intensity of the supernatant was close to zero. At pH 8.0, the deprotonated polymer collapsed because of the hydrophobic properties (insoluble in water); therefore, RhB could be entrapped in the particles. The total amount of RhB removed was calculated as about 0.758 mg.

The resulting RhB@$P_2P_1$@MSN composite was dispersed in an aqueous solution (5 mL, pH = 7.4, 0.05*M*), and then the five aliquot mixtures were placed in dialysis tubes (molecular weight cutoff = 14,000). This was followed by separate dialysis against five different kinds of external aqueous solutions. The particular conditions for each one are listed in Table I. At predetermined time intervals, 3 mL of external aqueous solution in the medium was taken out, and another 3 mL of fresh aqueous solution was added individually. The cumulative release concentrations of RhB were obtained through measurements of the fluorescence emission spectra.

The RhB loading capacity for $P_2P_1$@MSN was calculated by the following equation (m, the mass):

$$\text{RhB loading capacity } (\mu g/mg) = (m_{\text{RhB added to the solution}} - m_{\text{RhB removed}})/\text{Weight of the nanocomposites}$$

**Table I.** Five Different Kinds of External Aqueous Solutions (PBS, 0.05*M*) Used for Experiments

| | Temperature (°C) | Medium pH | Volume of the medium (mL) | Volume of the composite (mL) |
|---|---|---|---|---|
| 1 | 28 | 7.4 | 10 | 1 |
| 2 | 45 | 7.4 | 10 | 1 |
| 3 | 70 | 7.4 | 10 | 1 |
| 4 | 28 | 4.0 | 10 | 1 |
| 5 | 28 | 8.0 | 10 | 1 |

### MTT Assays

The cytotoxicity of the MSNs was observed by MTT assays in the COS7 cells. The cells were seeded in a 96-well plate with a density 6000 cells/per well and incubated 24 h in DMEM (100 $\mu$L) with 10% fetal bovine serum at 37°C and with 5% $CO_2$. Then, $P_2P_1$@MSN and MSN–$NH_2$ dispersed in DMEM were added to the wells. The concentrations ranged from 0 to 133.47 $\mu$g/mL. After they were co-incubated another 48 h, the medium was replaced with fresh medium (200 $\mu$L), and MTT (5 mg/mL, 20 $\mu$L) was introduced to each well for 4 h. Afterward, the medium was removed, and dimethyl sulfoxide (DMSO; 200 $\mu$L) was added to each well to dissolve the precipitated formazan violet crystals. The absorbance of formazan was monitored on a microplate reader (Bio-Rad, model 550) at 570 nm.

The relative cell viability was calculated on the basis of the following equation:

$$\text{Cell viability } (\%) = [(OD_{570(\text{sample})} - OD_{DMSO})/(OD_{570(\text{control})} - OD_{DMSO})] \times 100\%$$

$OD_{570(\text{sample})}$ was obtained from the absorbance of the medium incubated with cells and MSNs. $OD_{570(\text{control})}$ was obtained from the absorbance of the solution incubated with cells alone. OD is the abbreviation of optical density and in this part we got from the absorbance of different medium.

### Characterization

Fourier transform infrared (FTIR) spectra were performed on PerkinElmer spectrophotometer (USA). Thermogravimetric analysis (TGA) was detected through thermal analyzer (Thermo Gravimetric Analyzer, TGS-II, PerkinElmer). The morphology of the MSNs was viewed with scanning electron microscopy (SEM; FEI-Quanta 200) and high-resolution transmission electron microscopy [TEM; JEM-2100 (HR)]. For TEM measurement, the samples were dispersed evenly in ethanol. An acceleration voltage of 200 kV was applied. The suspension of particles was placed on a copper grid and dried at room temperature. The $\zeta$ potential, particle size, and size distribution of the MSNs were detected on a Malvern Nano-ZS ZEM3600 Zetasizer (United Kingdom). The surface area was measured with Brunauer–Emmett–Teller (BET). The pore size distribution was determined by the Barrete–Joyner–Halenda (BJH) method (ASAP2020, Micromeritics). Powder X-ray diffraction (XRD) patterns were recorded on a Bruker D8 instrument (Bruker Advance, Germany). X-ray photoelectron spectroscopy (XPS) was performed on an Kratos XSAM800 electron spectrometer with 253.6-eV Mg K$\alpha_1$ at 17 mA × 11.5 kV as the excitation source at $7 \times 10^{-7}$ Pa. Fluorescence analysis was performed on an RF-530/PC spectrofluorophotometer (Shimadzu).

## RESULTS AND DISCUSSION

### Preparation and Characterization of the MSNs

A schematic illustration of the synthetic route of $P_2P_1$@MSN is shown in Scheme 1. To prevent the modification of internal

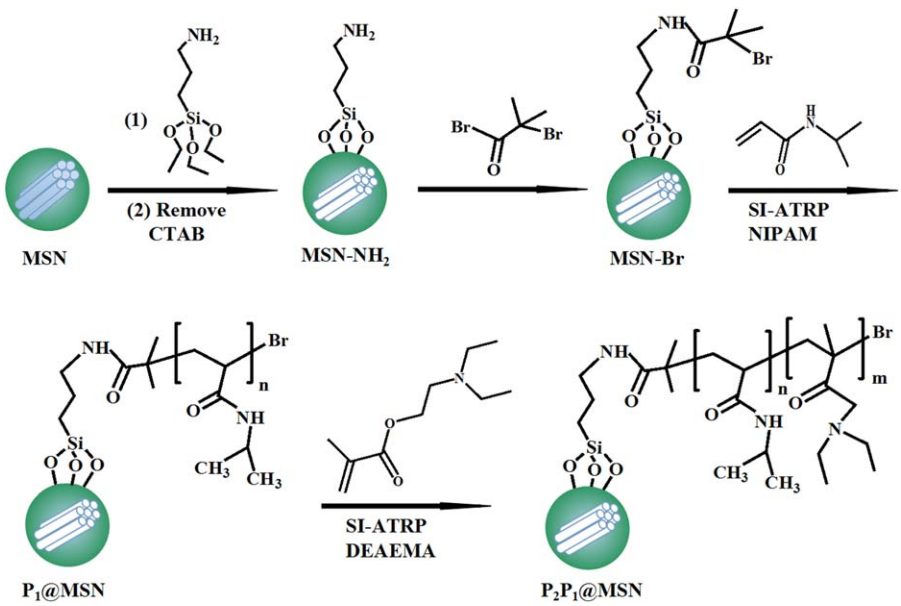


**Scheme 1.** Schematic illustration of the preparation of $P_2P_1$@MSN. [Color figure can be viewed in the online issue, which is available at wileyonlinelibrary.com.]

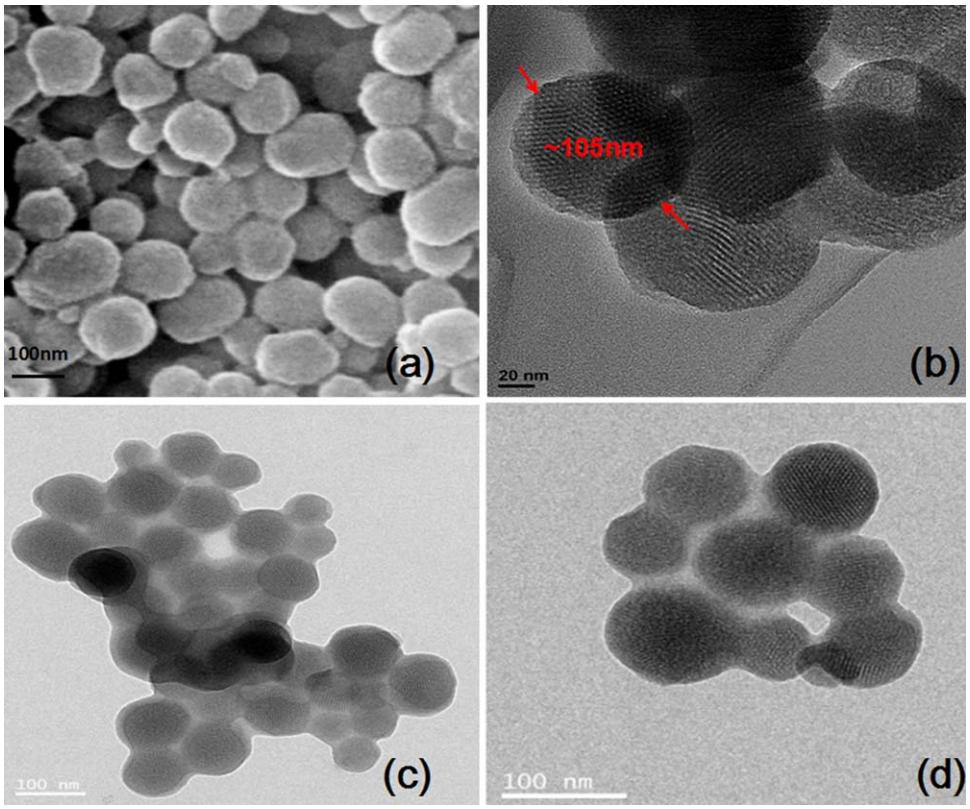


**Figure 1.** (a) SEM image of MSN–Br, (b) TEM image of MSN–Br, (c) TEM image of $P_1$@MSN, and (d) TEM image of $P_2P_1$@MSN. [Color figure can be viewed in the online issue, which is available at wileyonlinelibrary.com.]

channels,[41] APTES was introduced onto the surface of nanoparticles before the removal of the CTAB template. The BIBB initiators were connected to the particles through the reaction with amino group on the MSN surface. The block copolymer PDEAEMA-*b*-PNIPAM was grafted stepwise from the MSN surface through sustained SI-ATRP.

The diameter of the MSN with the ordered mesoporous structure was about 100–150 nm, as shown in Figure 1. As presented in the TEM images of $P_1$@MSN and $P_2P_1$@MSN [Figure 1(c,d)], polymer layers on the nanoparticles were observed after the modification of PNIPAM and PDEAEMA-*b*-PNIPAM. The polymer shells coated onto the MSNs were uniform, and the thickness of the shell was about 7 nm for $P_1$@MSN and about 16 nm for $P_2P_1$@MSN.

Small-angle XRD analysis was used to characterize the hexagonal array pore structure of the MSN. It was indexed as (100), (110), and (200) Bragg peaks[42] (as shown in Figure 2). The decreased intensity of the XRD diffraction peaks of $P_2P_1$@MSN [Figure 2(d)] were attributed to the introduction of polymers on the surface of the particles.[32]

The pore size and surface area of the MSNs were detected by BET and BJH analyses, respectively (Figure 3). The surface area and pore volume of MSN detected through BET and BJH analysis were 993.23 $m^2/g$ and 1.29 $cm^3/g$, respectively. A dramatic decrease in the BET surface area to 29.89 $m^2/g$ and a pore size of 0.15 $cm^3/g$ were observed for $P_2P_1$@MSN; this was attributable to the modification of the block polymer on the particles. As shown in the insert of Figure 3, the MSN had a narrow pore size distribution at 2.5 nm; this was big enough for RhB (1.6 nm) to transport freely.[43] The isotherm became flat after the modification of the polymer shell, and the pore diameter could not be obtained. This resulted from the covering of the polymer layer on the mesopores of the MSN.

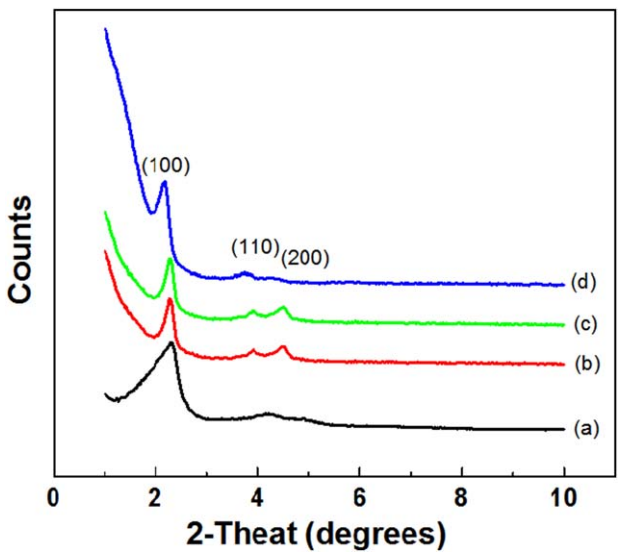


**Figure 2.** Powder XRD patterns of (a) MSN, (b) MSN–$NH_2$, (c) MSN–Br, and (d) $P_2P_1$@MSN. [Color figure can be viewed in the online issue, which is available at wileyonlinelibrary.com.]

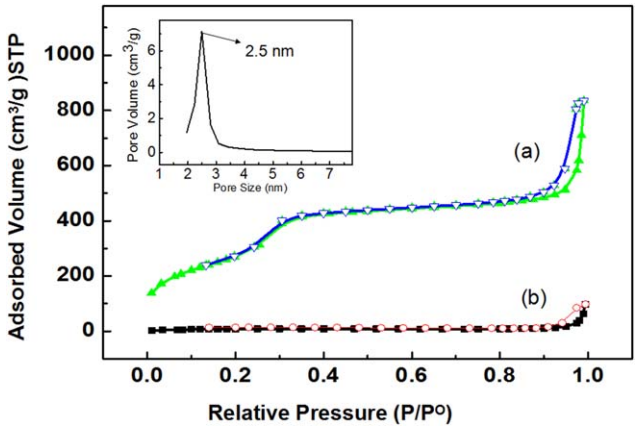


**Figure 3.** $N_2$ adsorption/desorption isotherms of (a) MSN and (b) $P_2P_1$@MSN. For curves a and b, the adsorption isotherms are denoted with solid symbols, and the desorption isotherms are marked with hollow symbols. P is equilibrium adsorptive pressure of $N_2$ and $P^0$ is the saturated vapor pressure of $N_2$ in adsorption/desorption temperature. The insert shows the BJH pore size distribution plot of MSN. [Color figure can be viewed in the online issue, which is available at wileyonlinelibrary.com.]

XPS was used to detect the chemical compositions of the MSNs during the modification steps. As shown in Figure 4(a), the Si, O, and C elements of MSN were observed. After the attachment of APTES, the new peak assigned to N at 403 eV proved the successful modification of amino group [as shown in Figure 4(b)]. Compared with the spectra of MSN–$NH_2$, the peaks of Br (74 and 187 eV) in the spectra of MSN–Br confirmed that the BIBB initiator was effectively introduced onto the MSN surface. After the modification of PNIPAM and PDEAEMA-*b*-PNIPAM, the intensity of the peaks belonging to C, N, and O were enhanced, and the intensity of the Br and Si signals dramatically decreased (as presented in Table S1, Supporting Information).

The FTIR spectra were also used to monitor the process of the surface modification of MSN, as shown in Figure 5. Typical

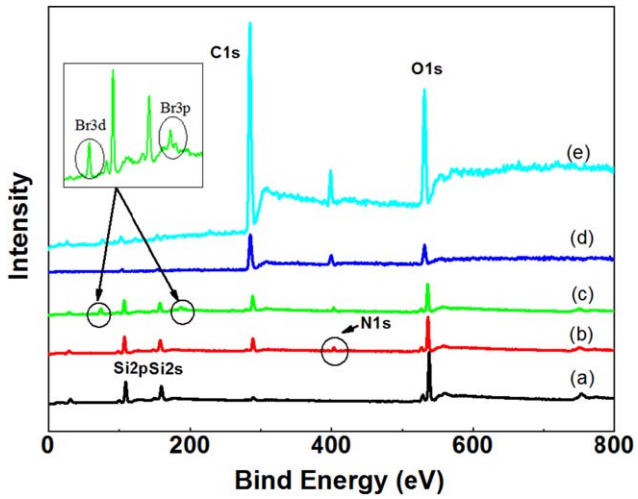


**Figure 4.** XPS spectra of (a) MSN, (b) MSN–$NH_2$, (c) MSN–Br, (d) $P_1$@MSN, and (e) $P_2P_1$@MSN. [Color figure can be viewed in the online issue, which is available at wileyonlinelibrary.com.]

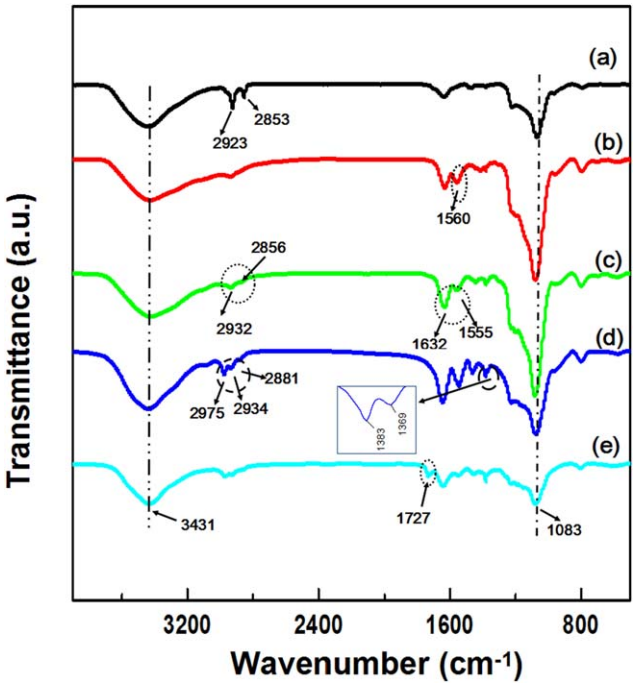


**Figure 5.** FTIR spectra of (a) MSN, (b) MSN–$NH_2$, (c) MSN–Br, (d) $P_1$@MSN, and (e) $P_2P_1$@MSN. [Color figure can be viewed in the online issue, which is available at wileyonlinelibrary.com.]

C—H stretching vibrations at 2923 and 2853 $cm^{-1}$ appeared because of the large amount of CTAB in MSN (Figure 5).[5] In Figure 5(b), 1560 $cm^{-1}$ was the typical absorption peak of $NH_2$. After the reaction between $NH_2$ and BIBB, the intensity of the absorption peaks at 1632 $cm^{-1}$ increased. The peak at 1632 $cm^{-1}$ belonged to amide I (1600–1690 $cm^{-1}$, C═O stretching), and the band at 1555 $cm^{-1}$ was attributed to amide II (1480–1575 $cm^{-1}$, N—H bending) [Figure 5(c)]. In the picture of $P_1$@MSN [Figure 5(d)], the characteristic double bonds at 1383 and 1365 $cm^{-1}$ were observed and were attributed to

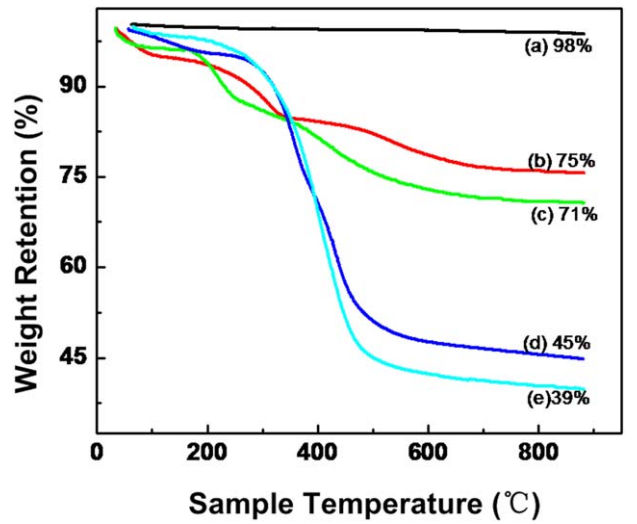


**Figure 6.** TGA curves of (a) MSN, (b) MSN–$NH_2$, (c) MSN–Br, (d) $P_1$@MSN, and (e) $P_2P_1$@MSN. [Color figure can be viewed in the online issue, which is available at wileyonlinelibrary.com.]

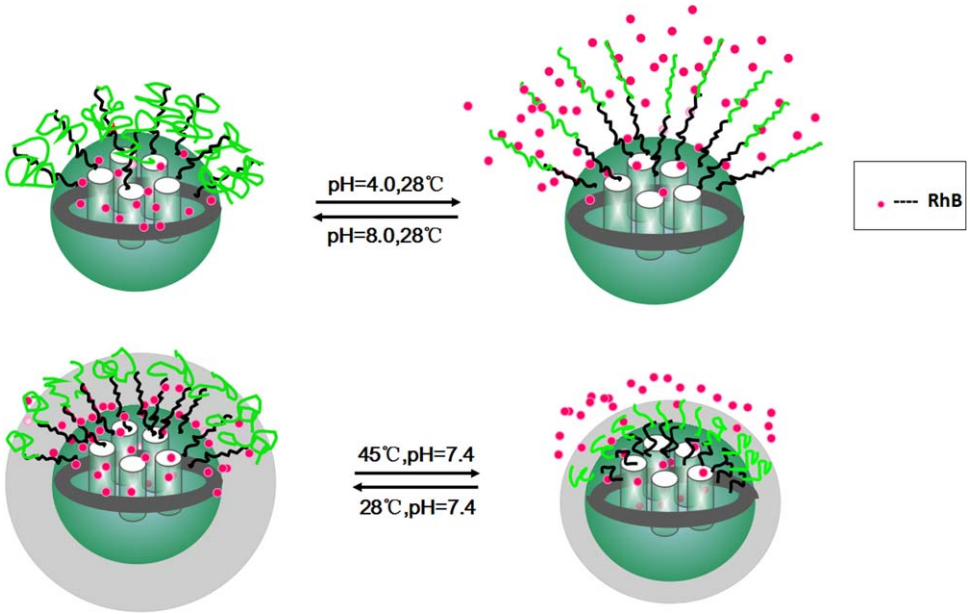


**Scheme 2.** Schematic representation for the stimuli-triggered release of RhB. [Color figure can be viewed in the online issue, which is available at wileyonlinelibrary.com.]

the introduction of isopropyl groups [$CH(CH_3)_2$]. In Figure 5(e), another new peak at 1727 $cm^{-1}$ emerged after the further polymerization of DEAEMA, as compared with Figure 5(d), which came from the stretching vibrations of carbonyl groups in the PDEAEMA.[32] These results indicated that the block copolymer PDEAEMA-*b*-PNIPAM was successfully grafted from the MSN surface.

TGA was used to estimate the weight percentages of polymers grafted on MSNs (Figure 6). The relatively low weight loss (temperature < 100°C) was mainly derived from the removal of water. The gradually increasing weight loss (temperature = 100–400°C) mainly came from the removal of different organic compounds. A sharp decomposition rate was observed at temperatures in the range between 400 and 800°C because of the thermal dehydroxylation of the internal surface silanol groups to form siloxane bridges and channel metamorphosis.[5] The weight losses of MSN, MSN–$NH_2$, MSN–Br, $P_1$@MSN, and $P_2P_1$@MSN were 2, 25, 29, 55, and 61%, respectively. The remarkable difference in weight losses between $P_2P_1$@MSN and MSN further demonstrated the successful modification of the polymers on the MSNs.

### Responsive Properties and Release Behaviors of the MSNs

The dynamic light scattering measurements were applied to investigate the responsive properties of the MSNs (Figure S2, Supporting Information). The hydrodynamic diameter of $P_2P_1$@MSN in PBS (pH = 7.4, 0.05*M*) was around 245 nm. The protonation of tertiary amine (soluble in aqueous solution) at low pH (4.0) led to an increase in the electrostatic repulsions and chain–solvent interactions among polymer chains. Consequently, the hydrodynamic diameter of $P_2P_1$@MSN increased to

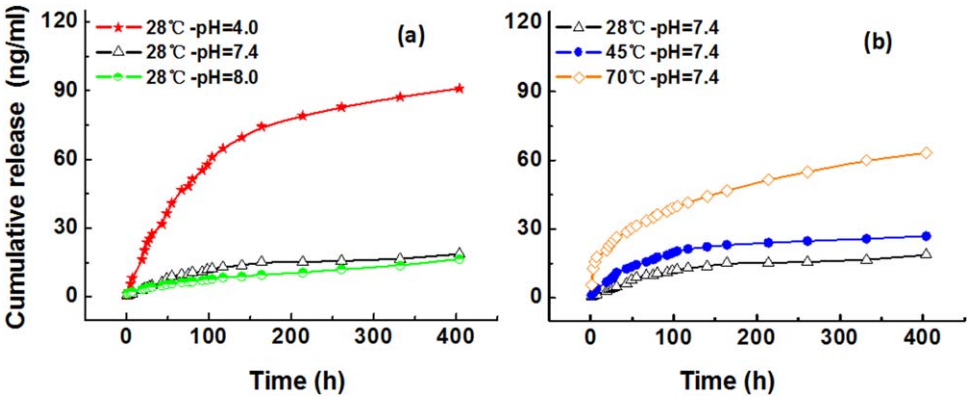


**Figure 7.** Cumulative release profiles of RhB from $P_2P_1$@MSN under different aqueous solution conditions (PBS, 0.05*M*): (a) pH and (b) temperature. [Color figure can be viewed in the online issue, which is available at wileyonlinelibrary.com.]

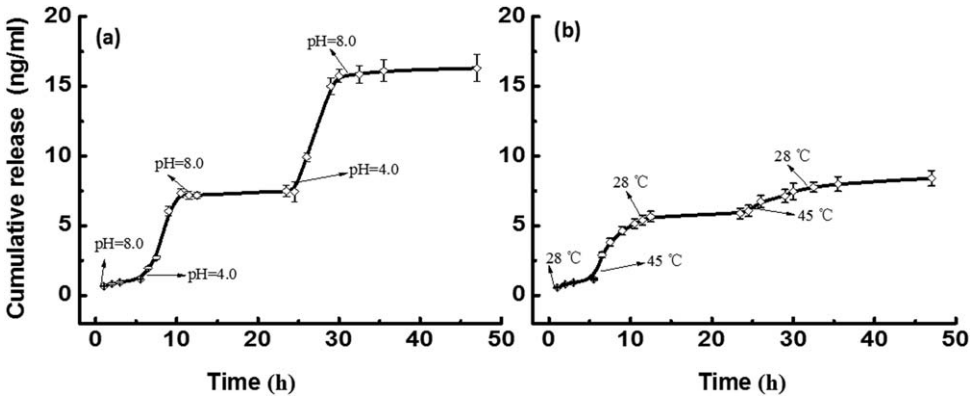


**Figure 8.** Cumulative release profiles of RhB from $P_2P_1$@MSN along with alternately changed solution conditions: (a) pH (between 4.0 and 8.0), 28°C, and 0.05*M* PBS and (b) temperature (between 28 and 45°C), pH = 7.4, 0.05*M* PBS.

319 nm. At pH 8.0, the deprotonation of PDEAEMA made the chain hydrophobic. The hydrophobic polymer chains were water-insoluble and collapsed together in aqueous solution. As a result, the hydrodynamic diameter of $P_2P_1$@MSN decreased to 150 nm.

To investigate the stimuli-responsive release of the model drugs from the well-defined MSNs, the hydrophilic RhB was selected (Scheme 2), and the loading capacity of $P_2P_1$@MSN was calculated as about 12 $\mu$g/mg. The loading capacity of the polymer-coated MSNs dropped down generally to some extent, as reported;[30,32] this might have originated from the resistance among the long polymer chains. The dual-stimuli-responsive release behaviors of $P_2P_1$@MSN were monitored via the fluorescence intensity of the released RhB in the medium. Depending on the calibration curves of RhB under different conditions (Figure S3, Supporting Information), the related concentrations of RhB were obtained. The release profiles of RhB are displayed in Figure 7. For the investigation of the pH-responsive release from the MSNs, the temperature of the medium was maintained at 28°C. As shown in Figure 7(a), after 400 h, the cumulative release concentration of RhB reached 90 ng/mL at pH 4.0, whereas only 14 ng/mL RhB could be detected at pH 8.0. The protonation of tertiary amine at low pH led to an increase in the electrostatic repulsions and chain–solvent interactions among the polymer chains. Consequently, the capped block copolymer chains adopted a highly extended conformation in the medium, and then the drug was released to the medium. At pH 8.0, the hydrophobicity of the PDEAEMA chain induced the chains to collapse together, and the pores of the MSNs could be sealed efficiently. The collapse of the polymer chain was confirmed from the decrease in the hydrodynamic diameters of $P_2P_1$@MSN at pH = 8.0 (Figure S2, Supporting Information).

The temperature-responsive release profiles of RhB from the MSNs are shown in Figure 7(b). Within 400 h, the cumulative release concentration of RhB was about 15 ng/mL at 28°C, and it reached to 60 ng/mL at 70°C. The PNIPAM chain collapsed and became insoluble when the temperature was greater than the LCST (32°C).[41] With increasing temperature, the extended polymer chains shrank rapidly. The fast release of RhB at higher temperatures might have been due to the enhanced volume contraction degree of the polymer shells. Furthermore, heating also accelerated the diffusion of RhB and contributed to the faster release. The desired release profiles could be achieved by changes in the temperature of the medium.

Another two experiments were conducted to clarify whether the release of RhB could be switched on and off repeatedly. We changed the pH (4.0 and 8.0) or temperature (28–45°C) of the solutions in turn, respectively. The release profiles accounting for the temperature and pH of the solution are shown in Figure 8. It exhibited a promoted release rate when the pH value of the solution dropped to 4.0, and a remarkable decrease in the release rate was shown as the pH value of the solution going back to 8.0 again [Figure 8(a)]. A similar behavior was presented in Figure 8(b) with the adjustment of temperature. The release amount of RhB shown in Figure 8(a,b) were 16.3 ± 1.0 and 8.3±0.6 ng/mL, respectively, after 50 h.

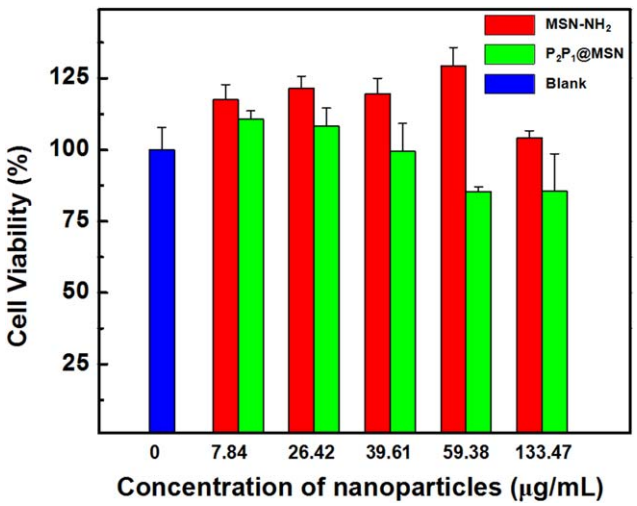


**Figure 9.** Cell viability of COS7 cells incubated with MSN–$NH_2$ and $P_2P_1$@MSN. [Color figure can be viewed in the online issue, which is available at wileyonlinelibrary.com.]

**Cytotoxicity of the MSNs**

We used MTT assays to investigate the cytotoxicity of MSN–$NH_2$ and $P_2P_1$@MSN. As shown in Figure 9, the MSN–$NH_2$ showed nearly no cytotoxicity to COS7 cells, even at a concentration of 133.47 $\mu$g/mL, and it could promote cell proliferation to some extent. For $P_2P_1$@MSN, the cell viability was higher than 85% at all of the designed concentrations and exceeded 100% at relatively lower concentrations. Therefore, the prepared drug-delivery system $P_2P_1$@MSN showed good biocompatibility.

## CONCLUSIONS

In summary, a temperature- and pH-responsive delivery system based on block copolymer PNIPAM-*b*-PDEAEMA capped MSNs was fabricated. The designed polymer shells endowed the materials with temperature- and pH-dependent properties in aqueous solution. The release of RhB from $P_2P_1$@MSN could be controlled by the adjustment of the temperature and the pH value of the medium. With the higher temperature and lower pH value of the medium, more model guests could be released from the MSNs; this was a long-time sustained release process. Moreover, the MTT assay showed that $P_2P_1$@MSN had good biocompatibility. The opening of the pores could be switched on and off as desired. This delivery system should have potential applications in the biomedical, anticorrosion, and antimicrobial fields.

## ACKNOWLEDGMENTS

The authors are grateful for financial support from National Natural Science Foundation of China (contract grant number 21204070).

## REFERENCES

1. Li, Y.; Gao, G. H.; Lee, D. S. *Adv. Healthcare Mater.* **2013**, *2*, 388.
2. Park, J. H.; Lee, S.; Kim, J.-H.; Park, K.; Kim, K.; Kwon, I. C. *Prog. Polym. Sci.* **2008**, *33*, 113.
3. Zhang, L.; Li, Y.; Yu, J. C. *J. Mater. Chem. B* **2014**, *2*, 452.
4. Panyam, J.; Labhasetwar, V. *Adv. Drug Deliv. Rev.* **2003**, *55*, 329.
5. Mathew, A.; Parambadath, S.; Park, S. S.; Ha, C. S. *Micropor. Mesopor. Mater.* **2014**, *200*, 124.
6. Wei, R.; Cheng, L.; Zheng, M.; Cheng, R.; Meng, F.; Deng, C.; Zhong, Z. *Biomacromolecules* **2012**, *13*, 2429.
7. Sawdon, A. J.; Peng, C. A. *Colloids Surf. B* **2014**, *122*, 738.
8. Yan, Q.; Wang, J.; Yin, Y.; Yuan, J. *Angew. Chem. Int. Ed.* **2013**, *52*, 5070.
9. Ren, T.; Wu, W.; Jia, M.; Dong, H.; Li, Y.; Ou, Z. *ACS Appl. Mater. Interfaces* **2013**, *5*, 10721.
10. Chiang, W. H.; Ho, V. T.; Huang, W. C.; Huang, Y. F.; Chern, C. S.; Chiu, H. C. *Langmuir* **2012**, *28*, 15056.
11. Huynh, C. T.; Nguyen, M. K.; Lee, D. S. *Macromolecules* **2011**, *44*, 6629.
12. He, C.; Kim, S. W.; Lee, D. S. *J. Controlled Release* **2008**, *127*, 189.
13. Allen, T. M.; Cullis, P. R. *Adv. Drug Delivery Rev.* **2013**, *65*, 36.
14. Barenholz, Y. *Curr. Opin. Colloid Interface Sci.* **2001**, *6*, 66.
15. Liu, R.; Zhang, Y.; Zhao, X.; Agarwal, A.; Mueller, L. J.; Feng, P. Y. *J. Am. Chem. Soc.* **2010**, *132*, 1500.
16. Sardan, M.; Yildirim, A.; Mumcuoglu, D.; Tekinay, A. B.; Guler, M. O. *J. Mater. Chem. B* **2014**, *2*, 2168.
17. Zhang, Z.; Balogh, D.; Wang, F.; Willner, I. *J. Am. Chem. Soc.* **2013**, *135*, 1934.
18. Patel, K.; Angelos, S.; Dichtel, W. R.; Coskun, A.; Yang, Y. W.; Zink, J. I.; Stoddart, J. F. *J. Am. Chem. Soc.* **2008**, *130*, 2382.
19. Radu, D. R.; Lai, C. Y.; Wiench, J. W.; Pruski, M.; Lin, V. S. Y. *J. Am. Chem. Soc.* **2004**, *126*, 1640.
20. Guardado-Alvarez, T. M.; Devi, L. S.; Vabre, J. M.; Pecorelli, T. A.; Schwartz, B. J.; Durand, J. O.; Mongin, O.; Blanchard-Desce, M.; Zink, J. I. *Nanoscale* **2014**, *6*, 4652.
21. Sun, J. T.; Yu, Z. Q.; Hong, C. Y.; Pan, C. Y. *Macromol. Rapid Commun.* **2012**, *33*, 81.
22. Guardado-Alvarez, T. M.; Sudha Devi, L.; Russell, M. M.; Schwartz, B. J.; Zink, J. I. *J. Am. Chem. Soc.* **2013**, *135*, 14000.
23. Gan, Q.; Lu, X.; Yuan, Y.; Qian, J.; Zhou, H.; Lu, X.; Shi, J.; Liu, C. *Biomaterials* **2011**, *32*, 1932.
24. Thomas, C. R.; Ferris, D. P.; Lee, J. H.; Choi, E.; Cho, M. H.; Kim, E. S.; Stoddart, J. F.; Shin, J. S.; Cheon, J.; Zink, J. I. *J. Am. Chem. Soc.* **2010**, *132*, 10623.
25. Wang, J.; Liu, H.; Leng, F.; Zheng, L.; Yang, J.; Wang, W.; Huang, C. Z. *Micropor. Mesopor. Mater.* **2014**, *186*, 187.
26. Chen, M.; He, X.; Wang, K.; He, D.; Yang, S.; Qiu, P.; Chen, S. *J. Mater. Chem. B* **2014**, *2*, 428.
27. Chen, F.; Zhu, Y. *Micropor. Mesopor. Mater.* **2012**, *150*, 83.
28. He, Q.; Gao, Y.; Zhang, L.; Zhang, Z.; Gao, F.; Ji, X.; Li, Y.; Shi, J. *Biomaterials* **2011**, *32*, 7711.
29. Zhang, J.; Niemela, M.; Westermarck, J.; Rosenholm, J. M. *Dalton Trans.* **2014**, *43*, 4115.
30. Liu, R.; Zhao, X.; Wu, T.; Feng, P. Y. *J. Am. Chem. Soc.* **2008**, *130*, 14418.
31. Muhammad, F.; Guo, M.; Qi, W.; Sun, F.; Wang, A.; Guo, Y.; Zhu, G. *J. Am. Chem. Soc.* **2011**, *133*, 8778.
32. Sun, J. T.; Hong, C. Y.; Pan, C. Y. *J. Phys. Chem. C* **2010**, *114*, 12481.
33. Xiao, D.; Jia, H. Z.; Zhang, J.; Liu, C. W.; Zhuo, R. X.; Zhang, X. Z. *Small* **2014**, *10*, 591.
34. Li, F.; Zhu, Y.; Wang, Y. *Micropor. Mesopor. Mater.* **2014**, *200*, 46.
35. Dong, L. L.; Peng, H. L.; Wang, S. Q.; Zhang, Z.; Li, J. H.; Ai, F. R.; Zhao, Q.; Luo, M.; Xiong, H.; Chen, L. X. *J. Appl. Polym. Sci.* **2014**, *131*, 40477.
36. Chen, X.; Soeriyadi, A. H.; Lu, X.; Sagnella, S. M.; Kavallaris, M.; Gooding, J. *J. Adv. Funct. Mater.* **2014**, *24*, 6999.
37. Huh, S.; Wiench, J. W.; Yoo, J. C.; Pruski, M.; Lin, V. S. Y. *Chem. Mater.* **2003**, *15*, 4247.

38. Yu, Q.; Zhang, Y.; Chen, H.; Wu, Z.; Huang, H.; Cheng, C. *Colloids Surf. B* **2010**, *76*, 468.
39. Yang, Y.; Yan, X.; Cui, Y.; He, Q.; Li, D.; Wang, A.; Fei, J.; Li, J. *J. Mater. Chem.* **2008**, *18*, 5731.
40. Kumar, S.; Tong, X.; Dory, Y. L.; Lepage, M.; Zhao, Y. *Chem. Commun.* **2013**, *49*, 90.
41. Mizutani, A.; Kikuchi, A.; Yamato, M.; Kanazawa, H.; Okano, T. *Biomaterials* **2008**, *29*, 2073.
42. Sun, Y. L.; Zhou, Y.; Li, Q. L.; Yang, Y. W. *Chem. Commun.* **2013**, *49*, 9033.
43. Zhuang, X.; Wan, Y.; Feng, C. M.; Shen, Y.; Zhao, D. Y. *Chem. Mater.* **2009**, *21*, 706.